

Evidence for continuing current in sprite-producing cloud-to-ground lightning

Steven C. Reising, Umran S. Inan and Timothy F. Bell

STAR Laboratory, Stanford University, Stanford, California

Walter A. Lyons

ASTeR Inc., Fort Collins, Colorado

Abstract. Radio atmospherics launched by sprite-producing positive cloud-to-ground lightning flashes and observed at Palmer Station, Antarctica, exhibit large ELF slow tails following the initial VLF portion, indicating the presence of continuing currents in the source lightning flashes. One-to-one correlation of sferics with NLDN lightning data in both time and arrival azimuth, measured with an accuracy of $\pm 1^\circ$ at $\sim 12,000$ km range, allows unambiguous identification of lightning flashes originating in the storm of interest. Slow-tail measurements at Palmer can potentially be used to measure continuing currents in lightning flashes over nearly half of the Earth's surface.

Introduction

Sprites are luminous glows in the mesosphere above thunderclouds extending between ~ 50 km and ~ 90 km altitude [Sentman *et al.*, 1995], and are believed to be produced as a result of the heating of lower ionospheric electrons by intense quasi-electrostatic fields which exist at high altitudes above thunderstorms following lightning discharges [Pasko *et al.*, 1995; 1996]. Although sprites occur in association with large positive-polarity cloud-to-ground (+CGs) lightning flashes [Boccippio *et al.*, 1995], the characteristics of +CGs which lead to their production is not yet known. In this work, we present new measurements at Palmer Station, Antarctica, of the radio atmospheric waveforms of lightning discharges associated with sprites. Results indicate that sprites are produced by those +CGs which excite radio atmospherics with an enhanced 'slow-tail' component, indicating the presence of continuing current in the CG flashes.

Radio atmospherics ('sferics') are impulsive electromagnetic signals launched into the earth-ionosphere waveguide by lightning discharges [Budden, 1961; pp. 5, 69], which can propagate with little attenuation, typically ~ 1 dB/Mm at > 1 Mm range [e.g., Davies, 1990; p. 389], and are thus observable at large distances (> 12 Mm) from the source. Arrival azimuth of sferics is determined using wideband VLF direction finding [Inan *et al.*, 1996].

At long ranges ($\sim 12,000$ km), sferics are repeatedly observed to have an oscillating VLF portion lasting ~ 1 ms, sometimes followed by two or three half-cycles of an ELF (< 600 Hz) slow tail (see Figure 1) [e.g. Hepburn, 1957; Taylor and Sao, 1970; Sukhorukov, 1992]. The VLF portion typically consists of the quasi-transverse-magnetic (QTM) modes in the earth-ionosphere waveguide, which have a cut-off frequency of ~ 1.6 kHz for a nighttime ionosphere [Sukhorukov, 1992]. The ELF slow tail is due to the transverse electromagnetic (TEM) mode, which does not have a cut-off frequency. Theoretical calculations show that the slow tail is excited at significant levels only by source lightning discharges with a continuing-current component with significant variations on the time scale of several milliseconds

[Wait, 1960]. The first half-cycle of the slow tail is delayed in time after the VLF onset by an amount related to the propagation distance [Wait, 1960; Sukhorukov, 1992]. Figure 1 shows examples of sferics originating in the same thunderstorm with (Figure 1b), and without (Figure 1a), a detectable slow tail as measured at Palmer. Note that the VLF peak amplitudes recorded at Palmer and the peak currents, as recorded by the National Lightning Detection Network (NLDN), of the two sferics shown are similar, while the ELF content is significantly different.

Description of the Experimental Data

The sferic waveforms are extracted from broadband ELF/VLF (~ 300 Hz to 22 kHz) recordings of the outputs from two orthogonal [labeled North-South (N/S) and East-West (E/W)] loop antennas at Palmer Station, Antarctica ($64^\circ 46' S, 64^\circ 03' W$, shown in Figure 2) [Inan *et al.*, 1996]. The digitally recorded (16-bit resolution) N/S and E/W wideband signals allow high resolution spectral and time-domain analysis of the sferic waveforms. In addition, the arrival azimuth directions are determined using VLF Fourier Goniometry [Inan *et al.*, 1996]. With B_{NS} and B_{EW} representing the outputs of the N/S and E/W antennas, the Fourier Goniometry method is based on the Fourier Transform of a function whose real part is B_{NS} and whose imaginary part is B_{EW} . The phase of the transform represents the direction of arrival as a function of frequency. The arrival azimuth of a given sferic is computed over the 5.5 kHz to 9.5 kHz band, weighted by the magnitude of the signal at each frequency. This frequency range is selected as one in which multiple cycles of the waveform are available within the duration of

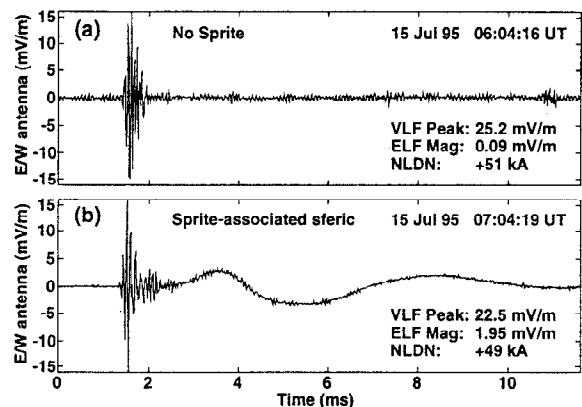


Figure 1. Waveforms of two sferics originating in the same midwestern U.S. thunderstorm with similar VLF intensities but markedly different ELF intensities. The waveform in Figure 1b exhibits a slow tail more than 20 times stronger than that of the one in Figure 1a. The sferic with the large slow tail (1b) was associated with an optically-recorded sprite, whereas the one without a measurable slow tail (1a) was not.

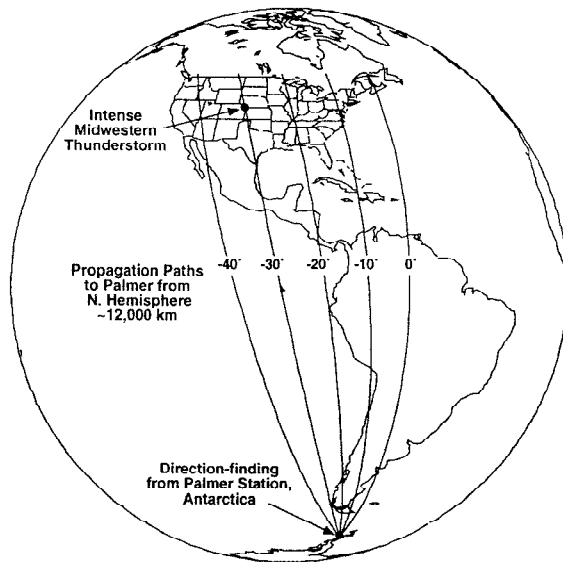


Figure 2. ELF/VLF broadband recordings are made at Palmer Station, Antarctica ($64^{\circ}46'S$, $64^{\circ}03'W$), at a range of $\sim 12,000$ km from the Nebraska and Iowa storms studied. Most of the Americas, the Atlantic and Pacific Oceans, Africa, and parts of Europe have smaller ranges to Palmer than the storms reported in this paper.

a single sferic and one which is relatively free of man-made and natural electromagnetic interference.

Slow-tail waveforms shown in this paper were analyzed by first lowpass filtering with a cutoff of 1 kHz. The 'slow-tail magnitude' was quantified as the average of the total magnetic field intensity $B = \sqrt{B_{NS}^2 + B_{EW}^2}$ over a period of 10 ms. Such a measure is appropriate in view of the fact that the initial ELF energy of the sferic at its source is dispersed by long-distance propagation.

The occurrence of sprites was determined on the basis of Low Light Level TV (LLTV) recordings made by ASTeR Inc. at Yucca Ridge Field Station ($40^{\circ}40'06''N$, $104^{\circ}56'24''W$). Images of sprites were recorded using two Xyberon model ISS-255 low-light imagers, sensitive from 400 to 900 nm, with a broad peak from 550 to 750 nm. Unfiltered lenses were used, including a Cosmocar f1.4 with a 12.5 mm focal length and a nominal $50\text{--}52^{\circ}$ horizontal field of view, depending upon elevation [Winckler *et al.*, 1996]. The sensing system had a face plate illumination sensitivity of 10^{-6} foot-candles. The EIA RS/170 video was recorded on SVHS, with the camera strapped to produce successive, independent 16.7 ms fields with IRIG-B time stamping from a GPS source.

Sprites observed at Yucca Ridge (YR) exhibited a large variety of shapes, multiplicity and duration, ranging from those lasting only for one video field (16.7 ms) to those which persisted for 15 video fields (251 ms), with the median duration being 3 video fields (50 ms). A field was included in a sprite event if sprite optical luminosity existed for any part of the 16.7 ms integration time. In cases where a 'sprite event' was observed in two or more successive fields, the shapes and distribution of individual elements often varied from field to field. A new sprite event (hereafter referred to as 'sprite') was identified on the basis of the presence of intervening video fields in which no sprites were observed.

In view of the limited field-of-view of the YR LLTV camera (Figure 3), the first step in the comparison of sprite and sferic data was the determination of which of the sferics observed at Palmer were launched by a CG flash within the field-of-view, as detected by NLDN. In one of the cases studied (Case B, see below), lightning flashes associated with 8 of the 29 sprites (28%) occurred just outside the LLTV field-of-view (see Figure 4). Each of these 8 sprites was observed by the LLTV camera; however, a portion of the sprite, as well as the causative lightning flash, was outside the LLTV

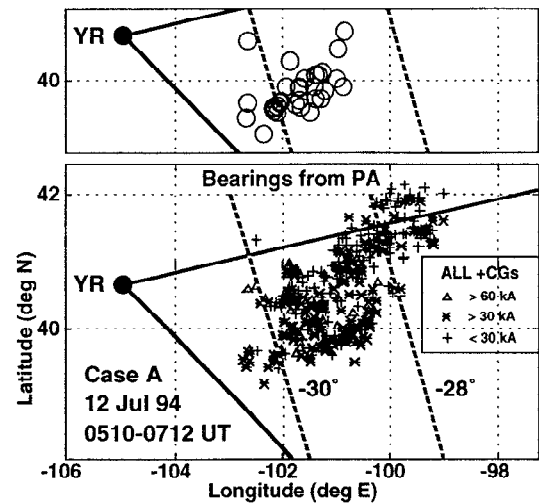


Figure 3. The lower panel shows all positive CG flashes recorded by NLDN from a mesoscale convective system in central/SW Nebraska and NE Colorado, from 0510-0712 UT on 12 July 94 (Case A). The locations of sprite-producing +CGs measured by NLDN within ± 100 ms of LLTV sprite events are denoted by circles in the upper panel. The outer edges of the LLTV camera fields-of-view are shown as segments extending from Yucca Ridge (YR).

field-of-view. In order to include these sprites in our statistics, the location criterion was extended to include all NLDN flashes which could have produced sprites anywhere in the field-of-view, even if the causative flash was just outside the nominal field-of-view.

The identification of sferic onset times with ~ 1 ms precision, the coordinated universal time (UTC) stamping of ELF/VLF data and the arrival azimuth estimates allow the one-to-one correlation of sferics with the first strokes of NLDN-recorded CG flashes. The sferics detected within the corresponding arrival azimuths at Palmer were required to occur within ± 2 ms of NLDN-recorded CG flashes within the field-of-view, after accounting for the propagation time (at nearly the speed of light) from the midwestern U.S. to Palmer. Figure 5 shows a histogram for Case A (discussed

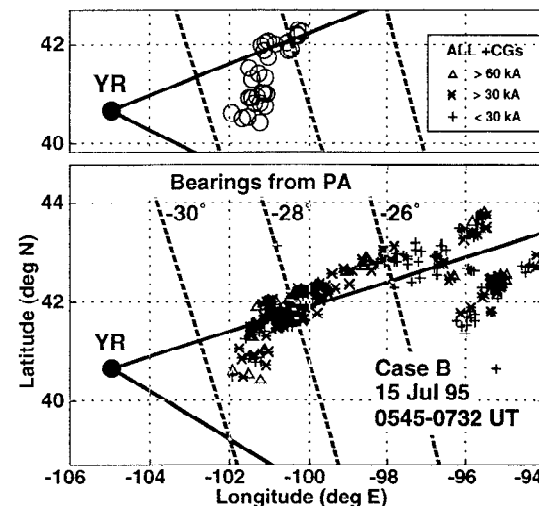


Figure 4. The lower panel shows the +CG flashes from 0545-0732 UT on 15 July 95 (Case B), an MCS with strong activity in central/SW Nebraska, with weaker +CGs in Iowa. The locations of sprite-producing +CGs are denoted by circles in the upper panel, as in Figure 3. The outer edges of the LLTV camera field-of-view are shown as segments extending from Yucca Ridge (YR).

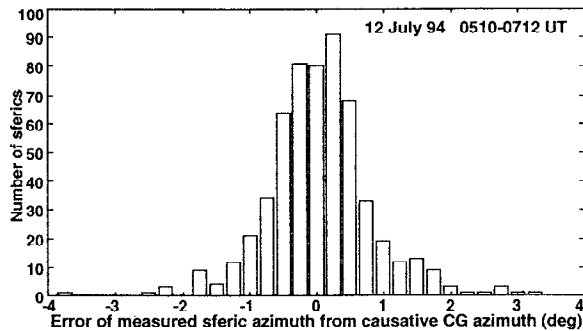


Figure 5. Histogram of error between arrival azimuths at Palmer Station (see Figure 2) using Fourier Goniometry and azimuths calculated from NLDN data. The NLDN location error is insignificant on this spatial scale.

below) of the error between the arrival azimuths at Palmer derived using Fourier Goniometry and the ‘true’ azimuths calculated from NLDN data. For over 90% of the sferics, the arrival azimuths as measured using Fourier Goniometry are within $\pm 1^\circ$ (± 200 km at 12,000 km range) of the measured NLDN flash locations.

Observations

Two different sprite-producing mesoscale convective systems (MCSs) over central and southwestern Nebraska (Figures 3 and 4) were studied. In Case A, on 12 July 94, 44 sprites were observed at YR between 0510 and 0712 UT, and in 31 of the 44 events (70%) the NLDN recorded +CG flashes within ± 100 ms of the period between the start time of the first video field and the end time of the last video field in which the sprite was recorded. Inspection of raw NLDN sensor data for the sprite event times without reported CGs indicates that CGs were seen by many sensors but were too complex to meet current NLDN CG acceptance criteria. These events produced inconsistent timing information, possibly due to contaminating intracloud activity or due to unusual return-stroke waveforms [K. Cummins, personal communication, 1996]. The sprite-associated NLDN CGs consisted of 52% single-stroke flashes and 39% two-stroke flashes, as compared to statistics for all +CGs in the storm of 74% single-stroke and 20% dual-stroke events. At Palmer, sferics were detected in association with 42 of the 44 (95%) sprites. The NLDN peak currents and ELF slow-tail magnitudes for the 31 NLDN-detected sprite-producing flashes are presented as the shaded areas in Figure 6a and 6b, respectively. The intensity distributions of a total of 328 NLDN-recorded +CG flashes within the LLTV camera field-of-view, as well as the slow-tail magnitudes of the corresponding 328 sferics observed at Palmer, are also shown in Figures 6a and 6b.

For Case B, on 15 July 95, between 0548 and 0732 UT, there were 35 sprite events observed at YR [Lyons, 1996], and 29 of the 35 (83%) had +CG flashes recorded by NLDN within the ± 100 ms criterion used in Case A. Of the sprite-associated NLDN flashes, 86% were single-stroke, 10% had two strokes and 3% had three, similar to the +CG statistics for the entire storm. At Palmer Station, sferics were recorded in association with 34 of the 35 (97%) sprites. The NLDN peak currents and ELF slow-tail magnitudes for the 29 NLDN-detected sprite-producing lightning flashes are respectively shown as shaded areas in Figures 6c and 6d. The unshaded bars show the distributions of the same two parameters for 184 NLDN-recorded +CG flashes and the corresponding sferics. ELF slow tails with magnitudes >1.5 mV/m were measured in time-correlation with two of the six sprites for which NLDN detected no +CG flashes.

For the 15 July 95 case, Figure 6 shows that slow-tail magnitudes measured at $\sim 12,000$ km range constitute a more definitive predictor of sprite occurrence than NLDN peak currents measured within ~ 400 km of the source lightning discharges. Large slow tails indicate that sprites are pro-

duced only by lightning with continuing current having significant magnitude variation on time scales of 1-5 milliseconds, consistent with model predictions [Pasko *et al.*, 1996], as discussed below.

In order to compare positive and negative CGs, we find the threshold above which 50% of the CG lightning produces sprites, i.e. 65 kA peak current and 1.5 mV/m slow-tail magnitude. In Case A, 24% of +CGs have peak currents >65 kA, whereas 4% of negative CGs (-CGs) exceed this threshold. In terms of slow-tail magnitudes, 18% of +CGs exceed the 1.5 mV/m threshold, and no -CGs have slow tails this large. Only 45% of the +CGs above the threshold are single-stroke events, compared to 74% of the +CGs in the overall storm.

In Case B, 12% of +CGs and only 0.6% of -CGs exceeded the peak current threshold of 65 kA. The ELF slow-tail threshold is exceeded by 11% of +CGs and only 0.3% of -CGs. Of that 11% of +CGs, 86% are single-stroke flashes, compared to 92% of +CGs in the entire storm. The only -CG exceeding the threshold was a single-stroke flash. The fact that very few -CGs have large slow tails (and thus continuing currents) is consistent with the absence of reports of -CGs in association with sprites, even though some -CGs may have peak currents as large as the largest +CGs which produce sprites. The smaller difference between the NLDN and slow-tail measurement statistics for -CGs in Case B in comparison to Case A indicates that slow-tail measurements of a larger number of storms are needed for further clarification. The few -CGs with slow tail magnitudes >1 mV/m show multiplicities similar to those of all -CGs in this storm.

Figure 7 illustrates the eight largest sferic slow-tail waveforms in Case B for sferics from sprite-producing lightning (Figure 7a) and for sferics not associated with sprites (Figure 7b). Both classes of sferics exhibit similar propagation characteristics, in their similar waveforms and ‘slow-tail separation’; defined as the time between the onset of the VLF sferic (defined as $t=0$) and the first slow-tail extremum. The different amplitudes of the waveforms are due to different excitation levels, specifically the magnitude of the continuing current [Wait, 1960]. The slow-tail separation is ~ 2 ms in Figure 6, in better agreement with the results of Wait [1960] than with Sukhorukov [1992], although this result could be due in part to the presence of an effective 300-Hz highpass filter in our recording system.

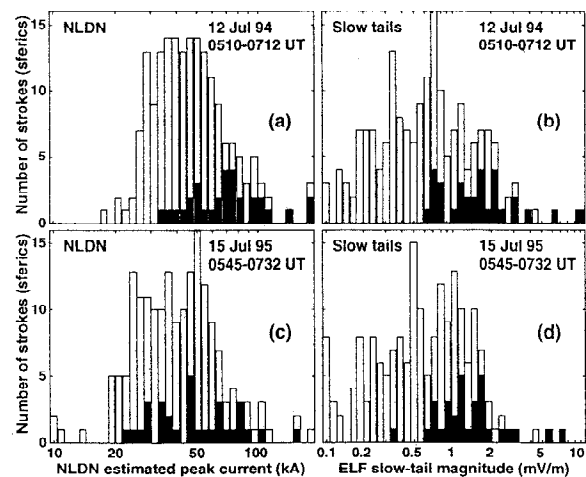


Figure 6. Distributions of NLDN peak current (a and c) and corresponding ELF slow-tail magnitudes (b and d) for all positive CGs within the LLTV camera field-of-view. The vertical scales are number of strokes (all first strokes) for the NLDN histograms (a and c), and number of sferics for the slow-tail histograms (b and d). Sprite-associated CGs are shown as shaded bars, and non-sprite-associated CGs are shown as unshaded bars. Case A histograms are shown at the top (a and b), and those for Case B are shown at the bottom (c and d).

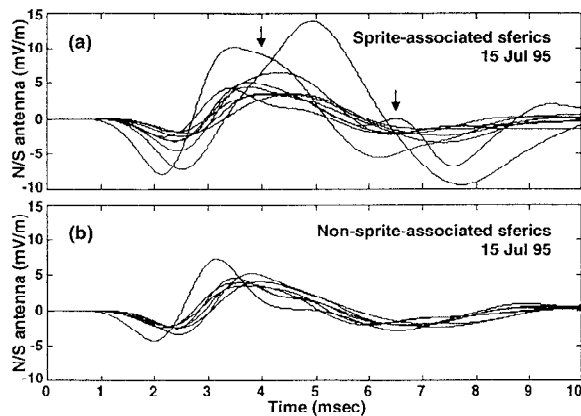


Figure 7. Sferic slow-tail waveforms of ELF/VLF broadband data recorded at Palmer and lowpass-filtered at 1 kHz. The waveforms are shifted in time such that their respective VLF onsets occur at $t = 0$ ms. a) The strongest 8 sferic slow tails from sprite-producing lightning. b) The strongest 8 sferic slow tails not associated with sprites. At times two sferics from different storms arrive at Palmer within the same ~ 10 ms. Arrows indicate examples of interfering sferic slow tails.

Summary and Discussion

ELF/VLF broadband measurements at Palmer Station, Antarctica, demonstrate the presence of continuing currents in sprite-producing +CG lightning flashes, as evidenced by the fact that sferics generated by these flashes exhibit large slow tails. It was shown for previous data sets [Boccippio *et al.*, 1995] that sprites are exclusively produced by +CG flashes with peak currents >50 kA; our data set contains sprite-producing +CGs with peak currents as low as 22 kA (see Figure 5). Our slow-tail measurements identify an additional characteristic exhibited by sprite-producing lightning discharges, namely continuing current. In this context, our results are consistent with the fact that many large +CG discharges do not lead to sprites and that those which do exhibit a wide range of peak currents. However, the fact that only 50% of +CGs with ELF slow-tail magnitudes greater than 1.5 mV/m produce sprites means that the occurrence of a positive CG with a large slow tail (or continuing current) is a necessary but not sufficient condition for production of sprites above the LLTV camera threshold. It is possible that the altitude of the thundercloud charge, as well as the dendritic structure of associated intracloud discharges, may also play controlling roles.

The experimental indication of the presence of continuing currents in sprite-producing CG flashes is consistent with our present state of understanding of the occurrence of sprites due to heating of ambient ionospheric electrons by intense quasi-electrostatic fields following lightning discharges [Pasko *et al.*, 1995; 1996; Boccippio *et al.*, 1995]. In the context of this mechanism, the important parameters that determine sprite occurrence are the altitude and magnitude of the thundercloud charge removed during a lightning discharge. For a fixed altitude of removed charge, the single most important parameter is the magnitude of charge, with the discharge duration playing a secondary role, as long as the charge removal time is less than the ionospheric response times of 1-10 ms [Pasko *et al.*, 1995; 1996; Boccippio *et al.*, 1995]. In the absence of continuing current, or for discharges lasting <1 ms, removal of large amounts (e.g. 200 Coulombs) of charge requires peak current levels of >200 kA, which are seldom observed [e.g. Brook *et al.*, 1982]. However, the rate of removal of thundercloud charge determines the altitude at which the maximum sprite brightness ('head') occurs [Pasko *et al.*, 1996].

The fact that sferic slow-tail characteristics of sprite-producing CG lightning discharges are measurable at 12,000

km distance from the thunderstorm regions offers promise for an assessment of occurrence of sprites on a global scale. As shown in Figure 2, most of the Western Hemisphere and Africa are within a similar range ($\sim 12,000$ km) to that of the storms studied from Palmer Station. Thus, ELF/VLF sferic waveform data measured at Palmer Station, Antarctica, and the accurate determination of arrival azimuths can allow the characterization of lightning continuing currents over nearly half the Earth's surface, especially when used in conjunction with satellite weather images.

Acknowledgments. The Stanford University component of this research was supported by the National Science Foundation under grant OPP-9318596 to Stanford University. The ASTeR, Inc. work was partially supported by NASA Kennedy Space Center under NAS10-12113. S. Reising was partially supported by NASA under grant NGT-30281, a NASA Graduate Student Fellowship in Earth System Science. The authors thank NASA's MSFC/DAAC for access to selected periods of NLDN lightning data.

References

- Boccippio, D. J., E. R. Williams, S. J. Heckman, W. A. Lyons, I. Baker, and R. Boldi, Sprites, ELF transients and positive ground strokes, *Science*, **269**, 1088, 1995.
- Brook, M., M. Nakano, P. Krehbiel, and T. Takeuti, The electrical structure of the Hokuriku winter thunderstorms, *J. Geophys. Res.*, **87**, 1207, 1982.
- Budden, K. G., *The Wave-Guide Mode Theory of Wave Propagation*, Logos Press, London, 1961.
- Davies, K., *Ionospheric Radio*, Pergamon, London, 1990.
- Hepburn, F., Atmospheric waveforms with very low-frequency components below 1 kc/s known as slow tails, *J. Atm. Terr. Phys.*, **10**, 266, 1957.
- Inan, U. S., S. C. Reising, G. J. Fishman and J. M. Horack, On the association of terrestrial gamma-ray bursts with lightning and implications for sprites, *Geophys. Res. Lett.*, **23**, 1017, 1996.
- Lyons, W. A., The Sprites '95 field campaign: Initial results - Characteristics of sprites and the MCSs that produce them, *Preprints*, 18th Conference on Severe Local Storms, American Meteorological Society, 442, 1996.
- Pasko, V. P., U. S. Inan, Y. N. Taranenko, and T. F. Bell, Heating, ionization and upward discharges in the mesosphere due to intense quasi-electrostatic thundercloud fields, *Geophys. Res. Lett.*, **22**, 365, 1995.
- Pasko, V. P., U. S. Inan, and T. F. Bell, Sprites as luminous columns of ionization produced by quasi-electrostatic thundercloud fields, *Geophys. Res. Lett.*, **23**, 649, 1996.
- Sentman, D. D., E. M. Wescott, D. L. Osborne, D. L. Hampton, M. J. Heavner, Preliminary results from the Sprites94 campaign: Red Sprites, *Geophys. Res. Lett.*, **22**, 1205, 1995.
- Sukhorukov, A. I., On the excitation of the Earth-ionosphere waveguide by pulsed ELF sources, *J. Atm. Terr. Phys.*, **54**, 1337, 1992.
- Taylor, W. L. and Sao, K., ELF attenuation rates and phase velocities observed from slow-tail components of atmospherics, *Radio Science*, **5**, 1453, 1970.
- Wait, J. R., On the theory of the slow tail portion of atmospheric waveforms, *J. Geophys. Res.*, **65**, 1939, 1960.
- Winckler, J. R., W. A. Lyons, T. E. Nelson and R. J. Nemzek, New high-resolution ground-based studies of sprites, *J. Geophys. Res.*, **101**, 6997, 1996.

S. C. Reising, U. S. Inan, T. F. Bell, STAR Laboratory, Stanford University, Stanford, CA 94305.
W. A. Lyons, 68040 Weld County Road 13, Ft. Collins, CO 80524

(received May 22, 1996; revised August 21, 1996; accepted September 6, 1996.)